



Article

Studies on the Removal of Phenol and Nitrophenols from Water by Activated Carbon Developed from Demineralized Kraft Lignin

Monika Chaudhary^{1,2}, Suhas^{1,*}, Sarita Kushwaha¹, Shubham Chaudhary¹, Inderjeet Tyagi³, Mohammad Hadi Dehghani^{4,5}, Baskaran Stephen Inbaraj^{6,*}, Joanna Goscianska⁷ and Minaxi Sharma⁸

¹ Department of Chemistry, Gurukula Kangri (Deemed to Be University), Haridwar 249404, India

² Department of Chemistry, Hariom Saraswati P.G. College, Dhanauri, Haridwar 247667, India

³ Centre for DNA Taxonomy, Molecular Systematics Division, Zoological Survey of India, Kolkata 700053, India

⁴ Department of Environmental Health Engineering, School of Public Health, Tehran University of Medical Sciences, Tehran 9821, Iran

⁵ Institute for Environmental Research, Center for Solid Waste Research, Tehran University of Medical Sciences, Tehran 9821, Iran

⁶ Department of Food Science, Fu Jen Catholic University, New Taipei City 24205, Taiwan

⁷ Department of Chemical Technology, Faculty of Chemistry, Adam Mickiewicz University in Poznań, Uniwersytetu Poznańskiego 8, 61-614 Poznań, Poland

⁸ Department of Applied Biology, University of Science and Technology, Ri-Bhoi, Meghalaya 793101, India

* Correspondence: suhasnatyan@yahoo.com (S.); sinbaraj@yahoo.com (B.S.I.)



Citation: Chaudhary, M.; Suhas; Kushwaha, S.; Chaudhary, S.; Tyagi, I.; Dehghani, M.H.; Stephen Inbaraj, B.; Goscianska, J.; Sharma, M. Studies on the Removal of Phenol and Nitrophenols from Water by Activated Carbon Developed from Demineralized Kraft Lignin. *Agronomy* **2022**, *12*, 2564. <https://doi.org/10.3390/agronomy12102564>

Academic Editor: Sung-Cheol Koh

Received: 1 September 2022

Accepted: 13 October 2022

Published: 19 October 2022

Publisher's Note: MDPI stays neutral with regard to jurisdictional claims in published maps and institutional affiliations.



Copyright: © 2022 by the authors. Licensee MDPI, Basel, Switzerland. This article is an open access article distributed under the terms and conditions of the Creative Commons Attribution (CC BY) license (<https://creativecommons.org/licenses/by/4.0/>).

Abstract: The present investigation deals with the importance of interaction and position of the nitro group in the adsorptive removal of 2-nitrophenol (2-NP), 4-nitrophenol (4-NP) and phenol by demineralized kraft lignin activated carbon (DKLAAC). The adsorption of phenol and NPs on DKLAAC was found to follow the order 2-NP > 4-NP > phenol. In this study, both solubility and donor–acceptor complex mechanism played an important role besides the porosity and surface area of the materials. Accordingly, the NP possessing the least solubility would noticeably exhibit a higher affinity to be adsorbed at the solid–liquid interface. Thus the highly hydrophobic 2-NP was adsorbed to a greater extent followed by 4-NP and phenol. Moreover, the adsorption capacity as affected by contact time, initial phenol concentration, pH, and temperature was also investigated. The experimental adsorption capacity by DKLAAC was 2.09, 2.34, and 2.20 mmol·g⁻¹ for phenol, 2-NP, and 4-NP at 25 °C, respectively, with the maximum amount being adsorbed within 40 min. The experimental data obtained for the removal of phenol and NPs were adequately fitted by the Langmuir adsorption isotherm and pseudo-second order kinetic models. Additionally, the temperature study revealed the adsorption process to be endothermic and spontaneous with high affinity between DKLAAC and phenols.

Keywords: activated carbon; adsorption; demineralized kraft lignin; isotherm; kinetics; phenols

1. Introduction

The contamination of water sources due to organic pollutants has become a serious concern in the last few decades [1]. These pollutants are found to have noxious impacts on humans due to their toxicity and carcinogenicity [2] and therefore their presence in the water systems is undesirable. Among organic pollutants, phenol and its derivative compounds have detrimental effects on living beings even at low concentrations owing to their poisonous, carcinogenic, mutagenic, and teratogenic nature and, therefore, the US Environmental Protection Agency has classified them as priority pollutants [3].

Various removal techniques such as ozonation [4], biological degradation [5,6], reduction [7], and adsorption [8] have been employed by the researchers for the removal of

phenols. Amidst these, adsorption employing different adsorbents such as clay [9], zeolites [10], metal organic frameworks [11], biomass [12], and activated carbon [8] have been used successfully by researchers. Adsorption is recognized as a versatile technique owing to its simplistic design and convenient operating technique [13–16] with activated carbons as the extensively utilized materials for the removal of phenol and its derivatives [8,17]. However, to understand the process better for the removal of molecules, the study of adsorbate–adsorbent interactions and the effect of groups is also necessary.

The chemical structures and presence of groups on the molecules are the determining factors which can play a crucial role in their removal. In order to demonstrate this, a study was carried out on the adsorption of phenol and nitrophenols by a microporous activated carbon (DKLAAC). The nitrophenols (NPs) have two functional groups, -OH, which acts as an activating group, and -NO₂, which behaves as a deactivating group [18,19]. Among these, the nitro group (-NO₂), being highly electronegative, withdraws π -electrons from the aromatic ring and, subsequently, the electron density of the accessible π -orbital permits 2-NP and 4-NP to interact with π -electrons on the adsorbent surface [20]. Furthermore, the role of nitro groups present in phenol is also important in the adsorption process since nitro groups are hydrophobic in nature, resulting in low aqueous solubility [21]. The adherent property of the phenolic molecules from aqueous media towards the surface of hydrophobic adsorbents mainly arises due to their dislike for water [22]. Besides nitro groups, phenol and NPs have -OH groups, which are polar in nature and help phenol molecules to form hydrogen bonding with the available functional groups on the adsorbent. Taken together, it can be said that two main adsorption mechanisms may be operating in a process: one due to the hydrophobicity between adsorbent and adsorbate and the other owing to the hydrogen bonding. Therefore, it is significant to understand the method of binding of these molecules for adsorptive removal of phenol and NPs. Moreover, it can facilitate easy prediction of the removal of noxious phenol and NPs if we know the role and binding nature of the existing functional groups.

Hence, the present study aimed to investigate a systematic comparison on the basis of functional groups for the adsorption of phenol, 2-NP, and 4-NP onto DKLAAC prepared in an oxidizing atmosphere. It is expected that the -NO₂ group present on phenol can play an important role and additionally its position is expected to make a difference in adsorption among them. Further, in order to compare the efficiency of DKLAAC, its precursor DKL and a commercial activated carbon (CAC) were also studied and reported herein. Moreover, the effect of various process parameters including contact time, initial phenol concentration, pH, and temperature which can affect the phenol and NPs adsorption on DKLAAC were also discussed.

2. Materials and Methods

All the reagents utilized in the current work were of analytical reagent (AR) grade. The adsorbates, phenol, 2-NP, and 4-NP were supplied by Sisco Research Laboratories Pvt. Ltd., Mumbai, India (SRL). The CAC and raw kraft lignin (RKL) samples were supplied by Rankem (Gujarat, India) and LignoTech Iberica (Cantabria, Spain), respectively. Double-distilled water was utilized to prepare the desired solutions.

The RKL was used as a precursor to prepare DKL and discussed in our previous work [23]. The activation was carried out by heating the DKL at 950 °C (rate of 8 °C min⁻¹; time: 30 min) in an oxidizing atmosphere. The details of the process are given in our previous work [23].

Stock solutions of phenol (1×10^{-2} mol·L⁻¹), 2-NP (5×10^{-3} mol·L⁻¹), and 4-NP (1×10^{-2} mol·L⁻¹) were prepared by dissolving 0.94, 1.39, and 1.39 g of phenol, 2-NP, and 4-NP, respectively in 1 L of distilled water. The different experimental solutions of desired concentrations were further obtained by dilution of the stock solution.

The adsorptive performance of DKLAAC towards phenol and NPs was analyzed by batch technique, in which, 10 mL of phenol (2×10^{-4} – 3.5×10^{-3} mol·L⁻¹), 2-NP (2×10^{-4} – 4.5×10^{-3} mol·L⁻¹), and 4-NP (2×10^{-4} – 4×10^{-3} mol·L⁻¹) solutions within

different stoppered glass tubes was added to 0.01 g of DKLAAC. The mixtures were then agitated continuously at 200 rpm and constant temperature (25 °C) in a water-bath shaking assembly (model 1201B, Ambala, India) to attain equilibrium. To study the effect of temperature on adsorption capacity, the adsorption isotherms in the above concentration range were developed for phenol, 2-NP, and 4-NP separately at three different temperatures (25 °C, 35 °C, and 45 °C). The measurement of the concentration of unadsorbed phenol and NPs at their respective maximum wavelength (λ_{\max}) of 268, 277, and 317 nm for phenol, 2-NP, and 4-NP was carried out using a Carry 60 UV-Vis spectrophotometer from Agilent (Santa Clara, CA, USA).

The amount of adsorbates adsorbed per gram of the adsorbent was calculated by using the following Equation (1):

$$q_e = \frac{(C_0 - C_e)V}{W} \quad (1)$$

where, C_0 ($\text{mol}\cdot\text{L}^{-1}$) is the initial concentration, C_e ($\text{mol}\cdot\text{L}^{-1}$) is the equilibrium concentration in solution, V is the volume of solution (L), W is the mass (g) of adsorbent used, and q_e ($\text{mol}\cdot\text{L}^{-1}$) is the amount of adsorbate adsorbed at equilibrium.

3. Results and Discussion

3.1. Effect of Contact Time and Initial Concentration

Equilibrium time plays a crucial role and is an important parameter that must be taken into the consideration to ensure the efficiency of the adsorbent. Therefore, to determine the time taken to reach the equilibrium for maximum adsorption of phenol, 2-NP, and 4-NP, the adsorption of adsorbates at a fixed concentration of $2 \times 10^{-3} \text{ mol}\cdot\text{L}^{-1}$ onto DKLAAC was studied (Figure 1A) as a function of contact time. This adsorbate concentration ($2 \times 10^{-3} \text{ mol}\cdot\text{L}^{-1}$) was chosen from the range of concentration used for developing adsorption isotherms. Results showed that initially the adsorption of phenol, 2-NP, and 4-NP was rapid and thereafter it reached equilibrium slowly. This is possibly owing to the ample vacant adsorption sites/pores and functional groups during the initial stage. Furthermore, less steric hindrance was felt by phenol and NPs while approaching the DKLAAC surface. However, a decrease in the adsorption was observed with time as compared with the initial stage owing to the reduced accessibility of vacant sites and enhancement in the steric hindrance by phenol and NPs molecules on DKLAAC [24,25]. Although the position of the $-\text{NO}_2$ group on phenol was thought to have an effect on the equilibrium, there was only a little difference observed in this case. It is clear from Figure 1A that the maximum amount of phenol, 2-NP, and 4-NP was removed within ~40 min attaining equilibrium at ~240 min [26]; therefore, a time span of 300 min was considered appropriate for all the studies to ensure equilibrium adsorption.

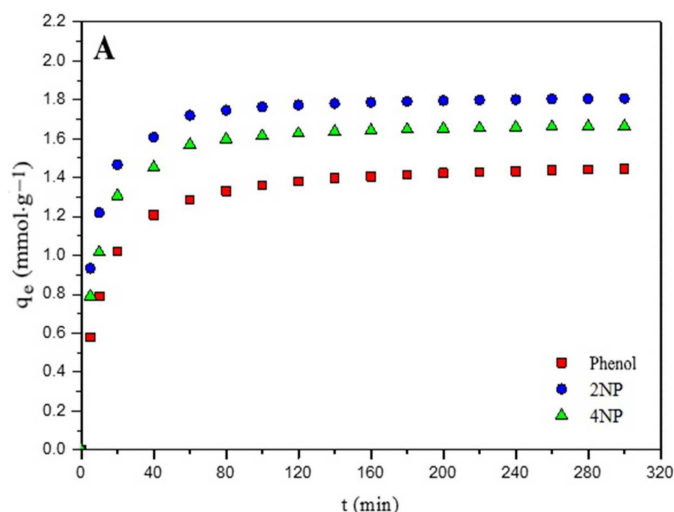


Figure 1. Cont.

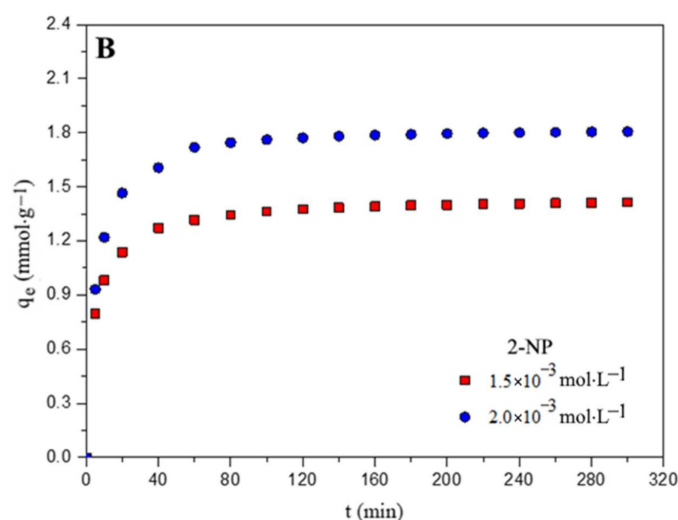


Figure 1. Effect of contact time on the adsorption of phenol, 2-NP and 4-NP on DKLAAC at 25 °C (A) and effect of initial concentration on adsorption of 2-NP on DKLAAC at 25 °C (B). An initial concentration of $2 \times 10^{-3} \text{ mol}\cdot\text{L}^{-1}$ was chosen for the study in (A), while two initial concentrations (1.5×10^{-3} and $2.0 \times 10^{-3} \text{ mol}\cdot\text{L}^{-1}$) were selected for 2-NP adsorption in (B).

The change in initial phenol/NPs concentration also alters the amount of the adsorption which was investigated at different concentrations (1.5×10^{-3} and $2.0 \times 10^{-3} \text{ mol}\cdot\text{L}^{-1}$). The results are presented in Figure 1B for 2-NP and similar plots observed also for phenol and 4-NP are shown in the Supplementary Material (Figures S1 and S2). The increase in the adsorption of phenol and NPs was observed with increase in the initial concentration [27]. This was because on increasing the initial concentration, the adsorbate molecules deliver the required driving force to reduce the mass transfer resistance between the adsorbent and adsorbates by concentration gradient effect [28,29].

3.2. Effect of Solution pH on Adsorption

The effect of pH of adsorbate solutions on their adsorption by DKLAAC was studied, since the pH of the aqueous solution is a critical factor in adsorption process. In order to investigate this effect, the adsorption parameters such as initial concentration, temperature, and contact time were kept constant during adsorption and the initial pH of the phenol and NPs was adjusted in the range of 2–12 using HCl (Himedia, Mumbai, India) or NaOH (SRL, Mumbai, India). The results of effect of pH on adsorption of phenol, 2-NP, and 4-NP on DKLAAC are shown in Figure S3 (Supplementary Material). Results showed that in the pH range of 2–8 for phenol and in the range 2–7 for 2-NP and 4-NP, a very small variation in the adsorption capacity of DKLAAC was observed, which may be attributed to the dispersion forces with small contribution of electrostatic forces in acidic solution [30]. The other reason for this small or no change in the adsorption is the amphoteric nature of DKLAAC which has a pH_{pzc} of ~ 7.5 . Interestingly, on the other hand, at higher pH the amount adsorbed decreased due to the repulsion between the negatively charged carbon surface and the phenolate/nitrophenolates. Moreover, the low adsorption at high pH is probably due to the presence of OH^- ions competing with the phenolates for the residual positively charged adsorption sites on the activated carbon surface [31]. Therefore all the experiments were carried out at pH 6–7 (neutral).

3.3. Effect of Temperature

In order to check whether the process is endothermic or exothermic and to compare the effect of temperature on removal of phenol and NPs on DKLAAC, experiments were performed at a temperature range of 25–45 °C (Figure 2A–C) and the results represented an increase in the amount of adsorption on DKLAAC from 2.09 to 2.27, 2.34 to 2.53, and 2.20 to 2.43 $\text{mmol}\cdot\text{g}^{-1}$ for phenol, 2-NP, and 4-NP, respectively with a rise in solution

temperature from 25–45 °C. This can be explained on the basis of diffusion of phenol and NP molecules throughout the outer surface and inside the pores of DKLAAC as well as decreased viscosity of the adsorbate solution [32–36]. Moreover, phenol and NPs usually form the H-bonds which are broken at high temperature and are responsible for the low solubility of the phenols, resulting in their higher affinity towards adsorbent surface [37]. Owing to these reasons, an increase in adsorption was observed with a rise of temperature, signifying the adsorption process to be endothermic in nature [34].

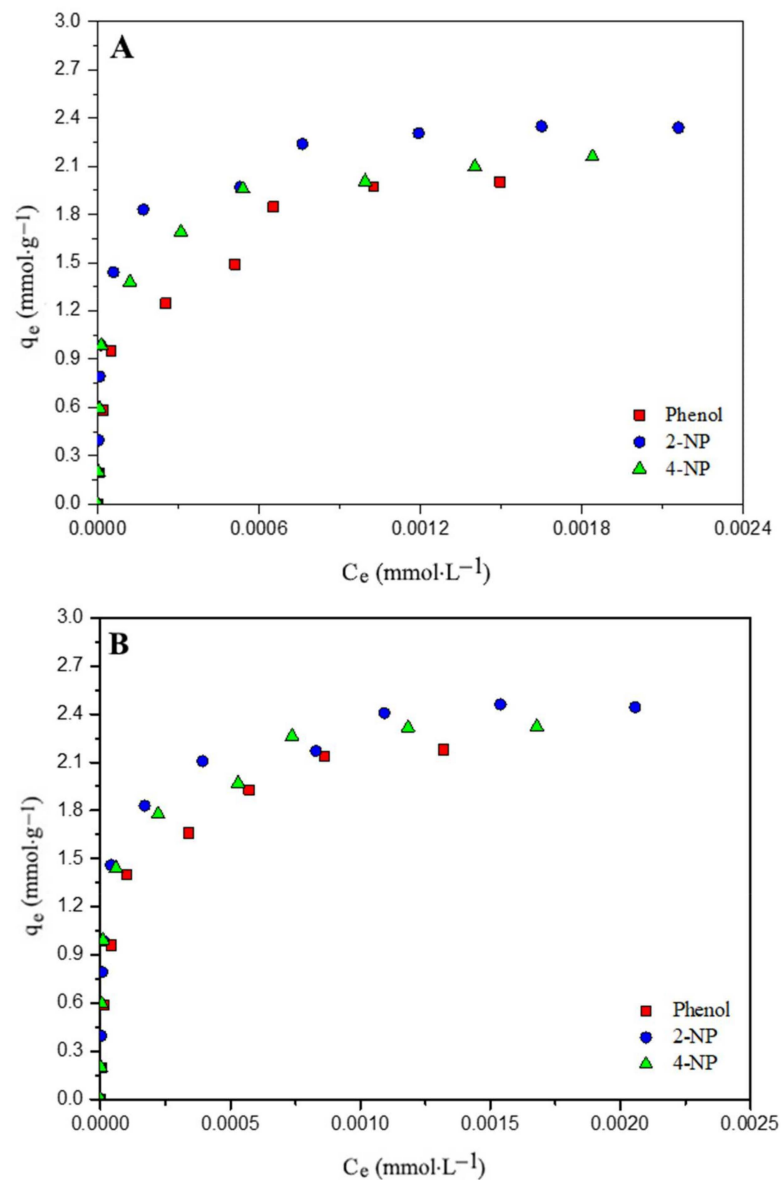


Figure 2. Cont.

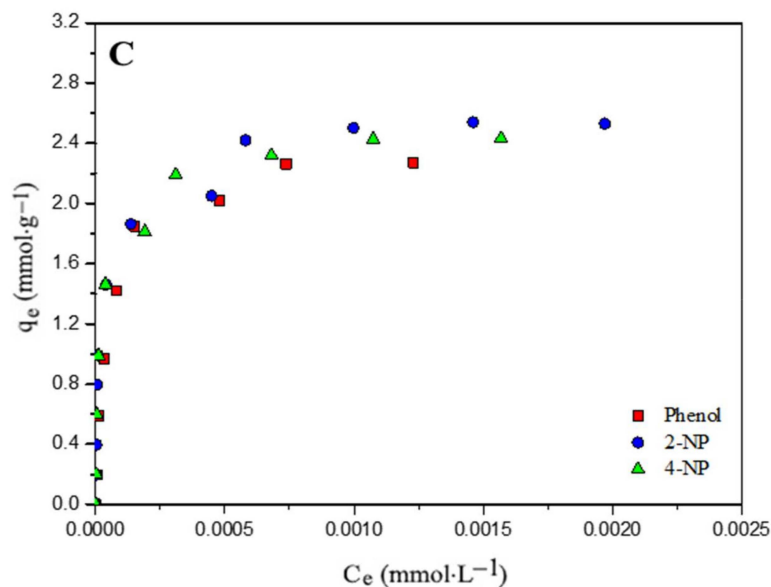


Figure 2. Adsorption isotherms for the removal of phenol, 2-NP, and 4-NP by DKLAAC at 25 °C (A), 35 °C (B), and 45 °C (C).

3.4. Adsorption Isotherms

Generally, on increasing the concentration of adsorbates, the adsorption increases and attains a saturation point from which the binding interactions between adsorbate and adsorbent can be estimated by using the adsorption isotherms. To investigate the impact of the presence of functional groups on the molecules in the adsorption process, the adsorption study of phenol, 2-NP, and 4-NP was carried out as a function of equilibrium concentration and the isotherms obtained are presented in Figure 2A–C. The maximum adsorbed amount (experimental, q_{exp}) on DKLAAC produced from DKL as elucidated from the adsorption isotherms (Figure 2A–C) were found to be 2.09, 2.34, and 2.20 $\text{mmol}\cdot\text{g}^{-1}$ for phenol, 2-NP, and 4-NP at 25 °C, respectively. It can be inferred from Figure 2A–C that the adsorption of phenol and NPs on DKLAAC follows the order 2-NP > 4-NP > phenol.

Moreover, to compare the impact of the role/position of the nitro group on the adsorption efficiency of DKLAAC, DKL (precursor to DKLAAC) and CAC were studied and the adsorption isotherms obtained for DKLAAC and CAC are shown in Figure 3A–C respectively for phenol, 2-NP, and 4-NP. Similar to the prepared DKLAAC, the removal of phenol and NPs on CAC also followed the order 2-NP > 4-NP > phenol. However, the amount of phenols adsorbed on CAC (surface area: $770 \text{ m}^2\cdot\text{g}^{-1}$) was observed to be relatively lower (1.14, 1.37, and 1.25 $\text{mmol}\cdot\text{g}^{-1}$ for phenol, 2-NP, and 4-NP, respectively) than DKLAAC at same temperature (25 °C) due to a more porous nature and high surface area (surface area: $1305 \text{ m}^2\cdot\text{g}^{-1}$) [38]. On the contrary, a negligible adsorption of phenol, 2-NP, and 4-NP was found on the surface of DKL because of its low surface area and therefore the Figure for the same is not shown.

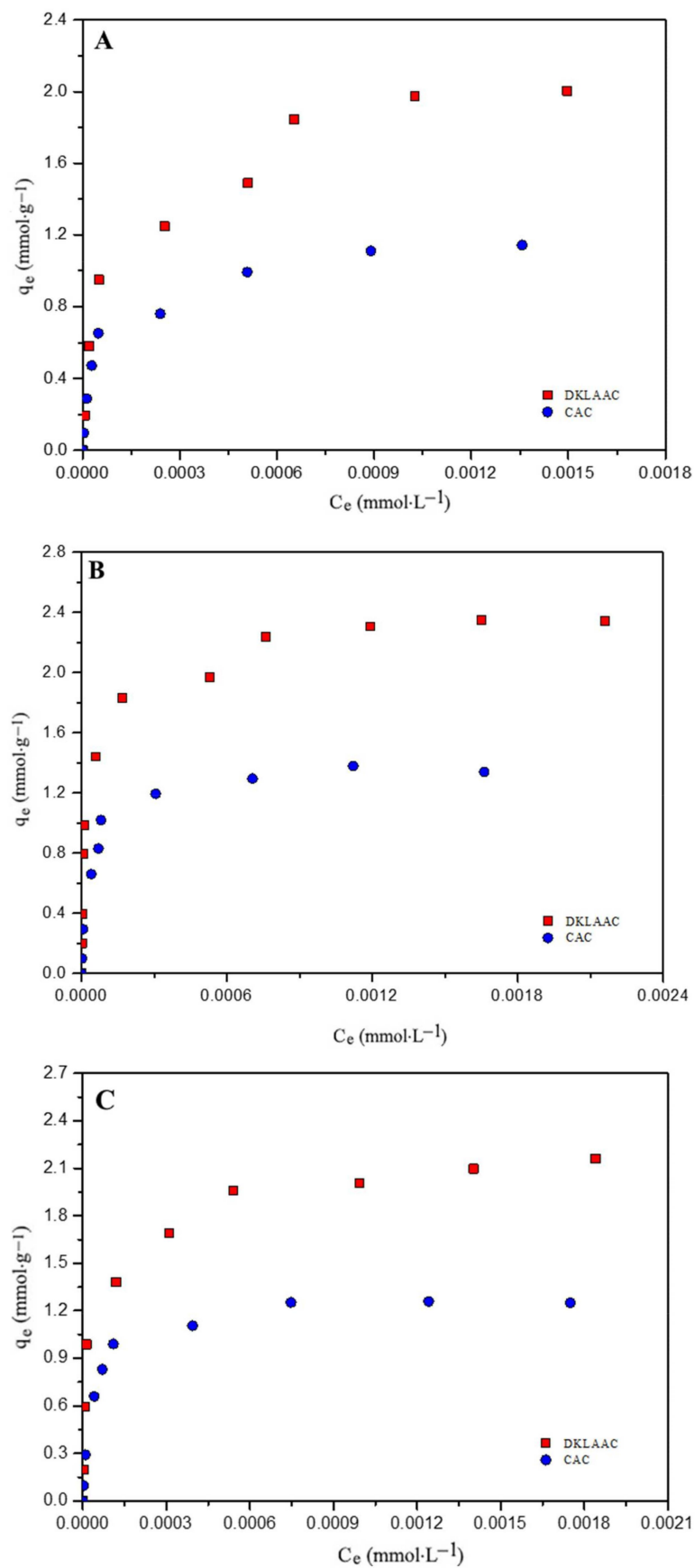


Figure 3. Adsorption isotherms for the removal of phenol (A), 2-NP (B), and 4-NP (C) by DKLAAC and CAC at 25 °C.

Isotherm models, namely, Langmuir, Temkin, Freundlich, and Dubinin–Radushkevich (D-R) were used for the analysis of experimental adsorption data obtained for the removal of phenol and NPs (Table 1).

Table 1. Experimental, Langmuir, Temkin, Freundlich, and D-R isotherm adsorption values for the removal of phenol and NPs on DKLAAC at three different temperatures (25 °C, 35 °C, and 45 °C).

Parameters	Phenol			2-NP			4-NP		
	25 °C	35 °C	45 °C	25 °C	35 °C	45 °C	25 °C	35 °C	45 °C
	Experimental								
q_{exp} (mmol·g ⁻¹)	2.09	2.18	2.27	2.34	2.46	2.53	2.2	2.32	2.43
q_{exp} (mg·g ⁻¹)	189	205	214	326	342	352	306	323	338
	Langmuir model								
q_{max} (mmol·g ⁻¹)	1.88	2.15	2.37	2.22	2.27	2.39	2.10	2.28	2.29
q_{max} (mg·g ⁻¹)	177	202	223	309	315	333	292	317	319
b (L·mol ⁻¹)	1.90×10^4	2.22×10^4	2.25×10^4	6.49×10^4	6.53×10^4	7.78×10^4	5.43×10^4	6.31×10^4	6.45×10^4
R^2	0.993	0.995	0.999	0.996	0.997	0.995	0.992	0.994	0.998
	Freundlich model								
K_f (mmol·g ⁻¹)	39.9	106	119	31.0	33.7	36.0	18.4	27.8	41.2
n	2.42	2.06	2.05	2.96	2.92	2.77	3.31	3.05	2.78
R^2	0.897	0.899	0.905	0.864	0.857	0.864	0.859	0.852	0.872
	Temkin model								
b (KJ·mol ⁻¹)	0.084	0.075	0.058	0.056	0.055	0.053	0.063	0.058	0.051
A_T (L·mg ⁻¹)	3.37	4.14	3.36	10.25	10.50	12.54	9.97	11.5	9.36
R^2	0.965	0.989	0.982	0.988	0.986	0.985	0.983	0.983	0.989
	D-R model								
E (KJ·mol ⁻¹)	1.25	1.57	1.73	2.01	2.04	2.24	1.83	2.03	2.06
q_m (mg·g ⁻¹)	119	116	121	217	219	231	213	226	230
R^2	0.886	0.914	0.890	0.895	0.894	0.909	0.909	0.907	0.887

The mathematical representation of the Langmuir equation (Equation (2)) [39] can be given as:

$$\frac{1}{q_e} = \frac{1}{q_{\text{max}}} + \frac{1}{q_{\text{max}}bC_e} \quad (2)$$

where, C_e and q_e are the equilibrium concentration and adsorbed amount of phenols respectively, b and q_{max} are the Langmuir constant and maximum adsorption capacity respectively. The plots of $\frac{1}{q_e}$ vs. $\frac{1}{C_e}$ for the adsorption of phenol, 2-NP, and 4-NP are drawn and shown only for 2-NP in Figure 4A, while the similar plots for phenol and 4-NP are provided in the supplementary material (Figures S4 and S5). The values of Langmuir capacity (q_{max}) were obtained from the intercept, whereas the adsorption constant b was assessed from the slope of the drawn plots (Table 1, Figures 4A, S4 and S5). A close comparison of the experimentally observed values and theoretically obtained values by the Langmuir model (Table 1) clearly shows the close proximity of both, thereby demonstrating the suitability of Langmuir isotherm model. Moreover, the constant 'b' which reflects the equilibrium constant and affinity of the process was evaluated (Table 1) and the values obtained for phenol, 2-NP, and 4-NP were found to be 1.90×10^4 , 6.49×10^4 , and 5.43×10^4 L·mol⁻¹, respectively, clearly indicating that the DKLAAC has a maximum affinity for 2-NP and minimum affinity for phenol.

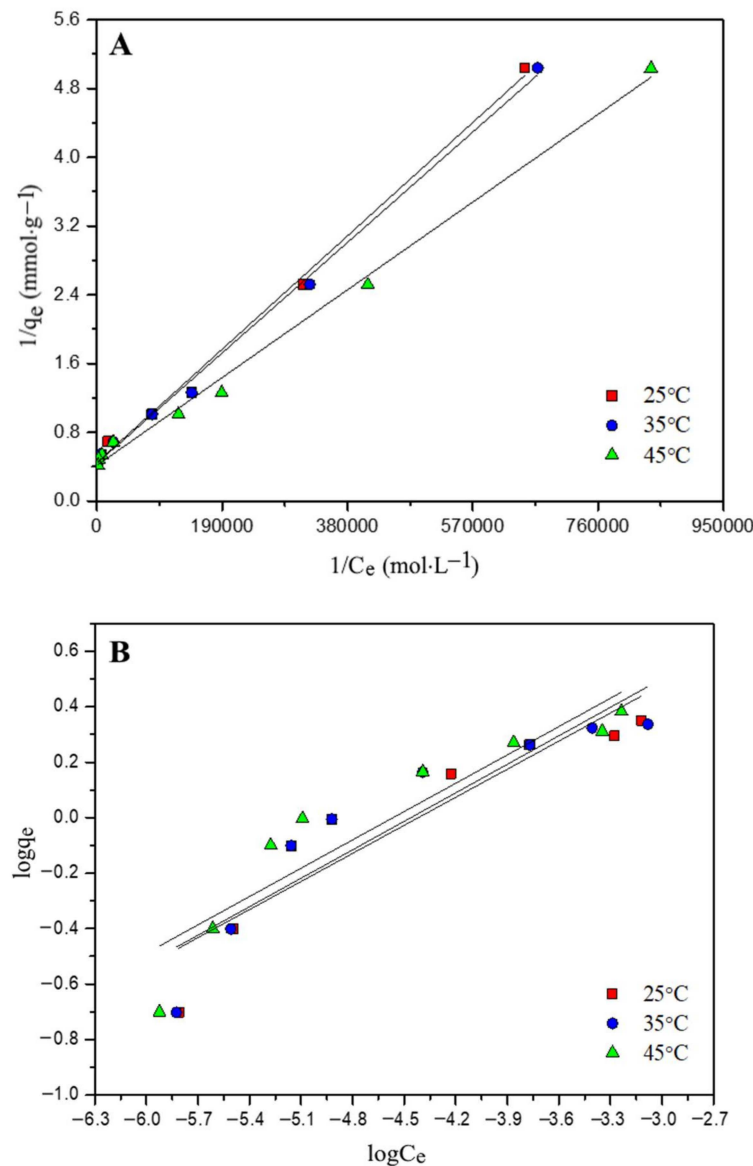


Figure 4. Langmuir (A) and Freundlich (B) adsorption isotherms of 2-NP on DKLAAC at different temperatures (25 °C, 35 °C, and 45 °C).

In addition to the Langmuir model, the data of phenol and NPs were also studied using the Freundlich model (Equation (3)) [40], which is represented as:

$$\log q_e = \log K_f + \frac{1}{n} \log C_e \quad (3)$$

where q_e denotes the adsorbed amount at the equilibrium, while K_f and n represent the adsorption capacity and heterogeneity factor, respectively. The Freundlich constants for the removal of phenol, 2-NP and 4-NP on DKLAAC were elucidated by plotting $\log q_e$ against $\log C_e$ with the plots for 2-NP at 25 °C, 35 °C, and 45 °C being shown in Figure 4B, while that for phenol and 4-NP shown respectively in Figures S6 and S7.

The Temkin model [41] that explains the adsorbate–adsorbent interactions was also studied and can be represented in a linear mathematical form (Equation (4)) as follows:

$$q_e = B_T \ln K_T + B_T \ln C_e \quad (4)$$

where, K_T ($L \cdot mg^{-1}$) and B_T (dimensionless) are the constants related to the Temkin isotherm binding constant, and the heat of adsorption, respectively, and B_T (Equation (5)) can be given by:

$$B_T = \frac{RT}{b_T} \tag{5}$$

where, T (K) is temperature, b_T ($J \cdot mol^{-1}$) is the Temkin constant and R is the universal gas constant ($R = 8.314 J \cdot mol^{-1} \cdot K^{-1}$). A plot of q_e versus $\ln C_e$ is shown only for 2-NP (Figure 5A), while that for phenol and 4-NP are shown in the Supplementary Material (Figures S8 and S9). The corresponding isotherm parameters obtained are given in Table 1.

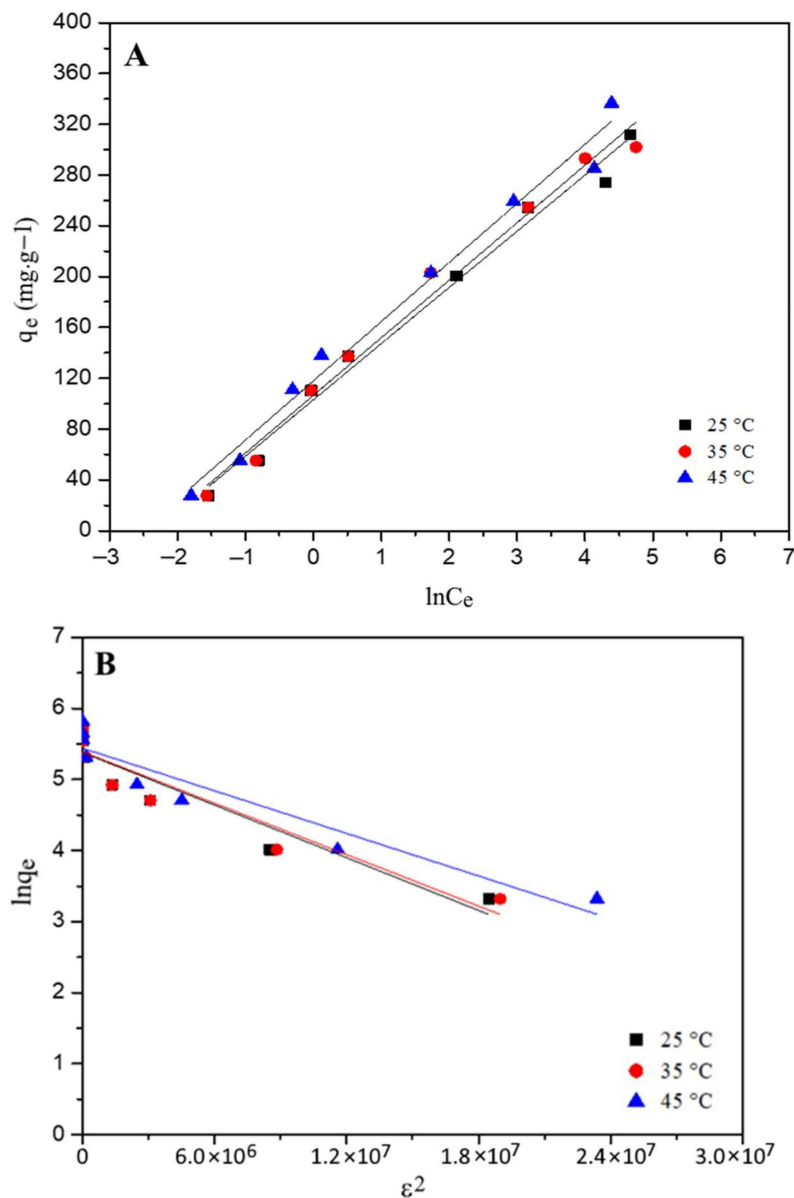


Figure 5. Temkin (A) and D-R (B) adsorption isotherms of 2-NP on DKLAAC at different temperatures (25 °C, 35 °C, and 45 °C).

The Dubinin–Radushkevich (D-R) model (Equations (6) and (7)) [42] was also used to illustrate the adsorption of phenols onto DKLAAC and can be given as:

$$\ln q_e = \ln q_m - \beta_{DR} \epsilon^2 \tag{6}$$

$$\varepsilon = RT \ln\left(1 + \frac{1}{C_e}\right) \quad (7)$$

where ε is the Polanyi potential, q_m ($\text{mg}\cdot\text{g}^{-1}$) is the D-R adsorption capacity, and β_{DR} ($\text{mol}^2\cdot\text{kJ}^{-2}$) is a constant which can be obtained from the mean free energy E ($\text{kJ}\cdot\text{mol}^{-1}$) by using equation $E = 1/\sqrt{2\beta_{\text{DR}}}$. The free energy parameter E helps to predict the nature of the process as either physisorption or chemisorption. The D-R model constants q_m and β_{DR} (Table 1) were obtained from the slope and intercept of the plots ($\ln q_e$ vs. ε^2) shown for 2-NP in Figure 5B as well as for phenol and 4-NP respectively in Figures S10 and S11 of the Supplementary Material. The comparison of correlation coefficients among different isotherm models tested (Table 1) clearly reveals the best applicability of the Langmuir model compared with the other investigated models. Similar adsorption isotherm behavior was also reported for the removal of phenols by activated carbon prepared from eucalyptus seed [43] and *Luffa cylindrica* [44].

The studies show that the extent and adsorption behavior of phenol and NPs are not only limited to the surface area and porosity of the adsorbent, but also to a variety of forces operating on the adsorption surface. Nevertheless, the functional groups attached to adsorbate molecules may also play a vital role in the adsorption process and thus cannot be ignored [45]. Therefore, in the present investigation, the role of the nitro groups and their position on the adsorption process were investigated. The order of adsorption capacity of phenol and NPs on DKLAAC (2-NP > 4-NP > phenol) confirmed the impact of the presence of nitro group (an electron-withdrawing group). Furthermore, it is expected that these ring-deactivating groups with decreasing electron density can undergo complex formation via the donor–acceptor mechanism and facilitate adsorption [46,47]. Other researchers [48] have also agreed to the fact that the phenol adsorption on the AC surface occurs through the donor–acceptor complex mechanism in which the aromatic ring of adsorbate and the carbonyl oxygen on carbon’s surface act as an acceptor and donor, respectively. Besides this, the H-bonding with hydrophilic sites/groups on AC surface generated during the activation period may also be effective in the adsorptive removal of phenol and NPs.

Another important parameter that can potentially influence the adsorption is the high hydrophobicity of adsorbate, which usually shows high affinity towards the AC surface [48]. Interestingly, this factor is also true in our case where hydrophobicity assists in promoting the adsorption of NPs owing to their poor solubility. Accordingly, 2-NP, being highly hydrophobic in character with least solubility, showed the maximum adsorption value (Table 1). Therefore, it may be suggested that a combined effect of solubility and donor–acceptor complex mechanism plays an important role in our study besides the surface area and porous nature of DKLAAC. A comparison of the adsorption capacities of different adsorbents employed by the researchers in the literature with DKLAAC is given in Table 2. A relatively high adsorption capacity and large surface area of DKLAAC demonstrate the impact of air activation technique involved in the preparation of DKLAAC.

Table 2. Comparison of adsorption capacities of different adsorbents with DKLAAC for the removal of phenol, 2-NP, and 4-NP as reported in the literature.

Adsorbent	Adsorbate	Surface Area	Adsorption Capacity ($\text{mg}\cdot\text{g}^{-1}$)	References
Oil palm shell-based activated carbon	phenol	988	168	[49]
Black wattle bark waste-based activated carbon	phenol	414	98.6	[50]
Rattan sawdust-based activated carbon	phenol	1083	149.25	[51]
Granular activated carbon	phenol	579.23	165.80	[52]
<i>Eucalyptus globulus</i> labill seed-based activated carbon	phenol	300	55.566	[53]
Magnetic activated carbon	phenol	942.9	107.5	[54]
DKLAAC	phenol	1305	177	This study

Table 2. Cont.

Adsorbent	Adsorbate	Surface Area	Adsorption Capacity (mg·g ⁻¹)	References
Raw winery residue based activated carbon	2-NP	227	376	[55]
Animal bone based char ash	2-NP	72.9	8.624	[56]
water hyacinth activated carbon	2-NP	-	47.62	[57]
Acid assisted multi wall carbon nanotube	2-NP	197.83	256.41	[58]
DKLAAC	2-NP	1305	309	This study
Granular activated carbon	4-NP	900	904.21	[59]
Cocoa shell-based activated carbon	4-NP	248.75	166.67	[18]
Granular activated carbon	4-NP	579.23	206.3	[52]
<i>Eucalyptus globulus</i> labill seed-based activated carbon	4-NP	300	137.005	[53]
DKLAAC	4-NP	1305	317	This study

3.5. Thermodynamic Studies

The thermodynamic parameters viz. change in enthalpy (ΔH°), free energy (ΔG°), and entropy (ΔS°), being significant to understand the feasibility, nature of the process, and spontaneity, must be determined to evaluate the adsorption process utilizing the following Equations (8) and (9):

$$\Delta G^\circ = -RT \ln b \quad (8)$$

$$\ln b = \frac{\Delta H^\circ}{RT} + \frac{\Delta S^\circ}{R} \quad (9)$$

where R (8.314 J·mol⁻¹·K⁻¹) is the universal gas constant and T and b are the temperature (°C) and thermodynamic equilibrium constant, respectively. The ΔH° and ΔS° were calculated from the $\ln b$ vs. $\frac{1}{T}$ plot and the values determined for these parameters are summarized in Table 3.

Table 3. Thermodynamic parameters for the removal of phenol and NPs on DKLAAC.

Phenols	Temperature (°C)	$-\Delta G^\circ$ (kJ·mol ⁻¹)	ΔS° (J·mol ⁻¹ ·K ⁻¹)	ΔH° (kJ·mol ⁻¹)
phenol	25	24.4	104.6	6.8
	35	25.6		
	45	26.5		
2-NP	25	27.5	116.1	7.1
	35	28.4		
	45	29.8		
4-NP	25	27.0	113.5	6.9
	35	28.3		
	45	29.3		

The positive values of the ΔH° , 6.8, 6.9, and 7.1 kJ·mol⁻¹ obtained for phenol, 2-NP, and 4-NP, respectively, indicate that the process follows an endothermic route, while its small magnitude specifies the physical adsorption (Table 3) [36]. Similar results were reported in the literature [22,59]. The observed endothermic behavior of the adsorption process may be due to the breaking of hydrogen bonds, resulting in enhanced adsorption at high temperatures as already discussed in the preceding paragraph. The negative ΔG° values (−24.4 to −29.8 kJ·mol⁻¹) confirm the spontaneity of the adsorption process and the range of the values indicates the process to be physisorptive in nature [60]. Table 3 also reveals that the ΔG° values increased on raising the temperature, suggesting the adsorption to be favorable at elevated temperatures. Nevertheless, the positive values of ΔS° are indicative of high affinity for the removal of phenols by DKLAAC. The thermodynamic results obtained were compared with other reported values for various adsorbents (Table 4) and were found to be comparable.

Table 4. Comparison of thermodynamic parameters of different activated carbons with DKLAAC for the removal of phenol and NPs as reported in the literature.

Adsorbent	Adsorbate	Free Energy (kJ·mol ⁻¹)	Enthalpy (kJ·mol ⁻¹)	Entropy (J·mol ⁻¹ ·K ⁻¹)	Reference
Carbon slurry-based activated carbon	phenol	−23.0	1.1	80.9	[22]
Magnetic activated carbon	phenol	−8.12	43.57	173.14	[54]
Sludge-based activated carbon	phenol	−5.33	16.52	105	[61]
Black wattle bark-based activated carbon	phenol	−12.20	7.89	70	[50]
DKLAAC	phenol	−24.4	6.8	104.6	This study
Granular activated carbon	2-NP	−3.30	5.92	90	[59]
Raw winery residue-based activated carbon	2-NP	−17.35	−5.53	30	[55]
Tucuma seed-based carbon activated with ZnCl ₂ (1:1)	2-NP	−16.66	105.40	405.2	[62]
Tucuma seed-based carbon activated with ZnCl ₂ (1:1.5)	2-NP	−16.89	50.18	224.9	[62]
Tucuma seed-based carbon activated with ZnCl ₂ (1:2)	2-NP	−17.76	36.30	181.3	[62]
DKLAAC	2-NP	−27.5	7.1	116.1	This study
Pine sawdust-based Activated carbon	4-NP	−4.31	13.068	49.908	[63]
Orange waste peel-based activated carbon	4-NP	−21.10	7.78	95	[64]
Granular activated carbon	4-NP	−10.48	11.00	20	[59]
Coconut shell-based granular activated carbon	4-NP	−5.17	6.02	38.18	[65]
<i>Luffa cylindrica</i> fruit-based activated biochar	4-NP	−26.84	17.54	145	[44]
DKLAAC	4-NP	−27.0	6.9	113.5	This study

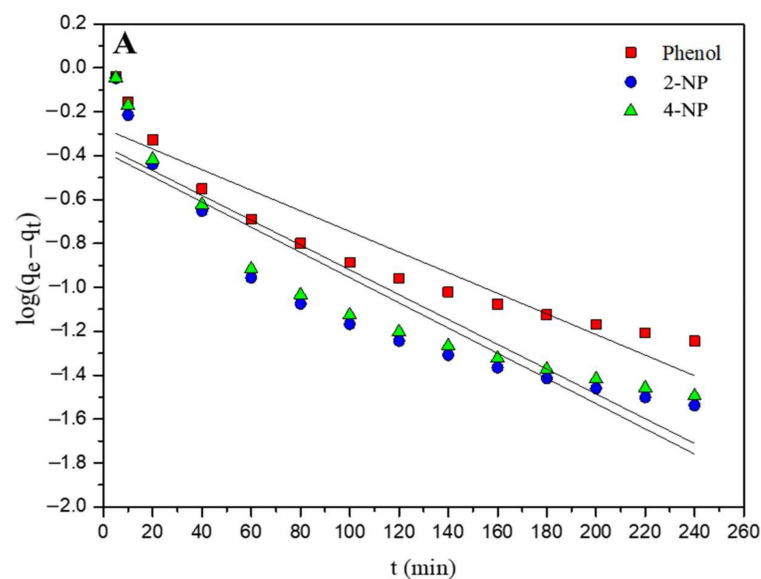
3.6. Kinetic Studies

Kinetic investigations were carried out to discover more about the adsorption of phenol and NPs (differentiated on the basis of their position) on DKLAAC and the data were tested using various well-known models.

The pseudo-first order (PFO) equation by Lagergren [66] suggested that the kinetics of adsorption of the adsorbate from aqueous solution can be represented as shown below (Equation (10)):

$$\log(q_e - q_t) = \log q_e - \frac{k_1}{2.303} t \quad (10)$$

where q_e and q_t are the adsorbed amount of phenols at equilibrium and at time t , respectively. k_1 is the Lagergren rate constant for the PFO equation. The model was applied and the values of q_e (from slope) and k_1 (from intercept) were evaluated from the curves plotted between $\log(q_e - q_t)$ and t (Figure 6A). The obtained values are presented in Table 5.

**Figure 6.** Cont.

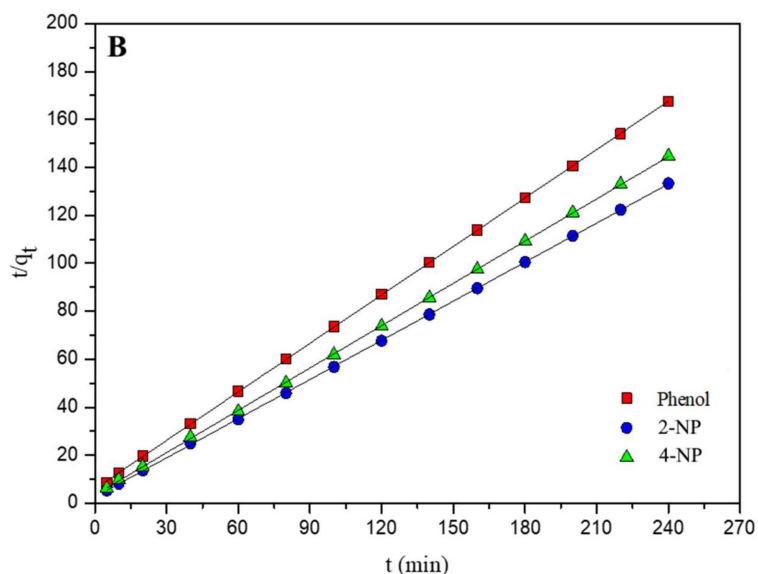


Figure 6. PFO (A) and PSO (B) kinetic plots for the removal of phenol, 2-NP, and 4-NP by DKLAAC at 25 °C with the initial phenol concentration at 2×10^{-3} mol·L⁻¹.

Table 5. Kinetic parameters for the removal of phenol and NPs on DKLAAC.

Parameters	Phenol	2-NP	4-NP
Experimental			
C ₀ (mol·L ⁻¹)	2×10^{-3}	2×10^{-3}	2×10^{-3}
q _{e(exp)} (mmol·g ⁻¹)	1.49	1.83	1.69
PFO			
q _{e(cal)} (mmol·g ⁻¹)	0.530	0.416	0.442
K ₁ (min ⁻¹)	0.011	0.013	0.013
R ²	0.900	0.855	0.858
PSO			
q _{e(cal)} (mmol·g ⁻¹)	1.48	1.84	1.70
K ₂ (g·mmol ⁻¹ ·min ⁻¹)	0.076	0.112	0.100
R ²	0.999	0.999	0.999
IPD			
K _{id1}	0.152	0.160	0.162
C ₁	0.284	0.659	0.487
R ²	0.969	0.914	0.937
K _{id2}	0.022	0.016	0.018
C ₂	1.11	1.57	1.41
R ²	0.900	0.742	0.752
Elovich			
α (mmol·g ⁻¹ ·min ⁻¹)	0.999	8.05	3.15
β (g·mmol ⁻¹)	4.66	4.84	4.67
R ²	0.952	0.908	0.917

PFO: Pseudo-first order; PSO: Pseudo-second order; IPD: Intraparticle diffusion model.

Besides PFO, the pseudo-second order (PSO) [67] model was also utilized to analyze the kinetics of the process and can be described as shown below (Equation (11)):

$$\frac{t}{q_t} = \frac{1}{k_2 q_e^2} + \frac{1}{q_e} t \tag{11}$$

where q_t and q_e are the adsorbed amount of phenols at time t and equilibrium, respectively. k_2 is the equilibrium rate constant for the PSO equation. To evaluate the applicability of the PSO adsorption model, t/q_t was plotted as a function of time (Figure 6B), whereas the values obtained from the graphs are given in Table 5.

Furthermore, the Elovich Equation [68] was also used for the analysis of the experimental adsorption data and is given as follows (Equation (12)):

$$q_t = \frac{1}{\beta} \ln(\alpha\beta) + \frac{1}{\beta} \ln(t) \tag{12}$$

where, q_t ($\text{mmol}\cdot\text{g}^{-1}$) is the amount adsorbed at time t (min), α ($\text{mmol}\cdot\text{g}^{-1}\cdot\text{min}^{-1}$) is the constant for initial adsorption, β ($\text{g}\cdot\text{mmol}^{-1}$) is the rate constant linked to the extent of surface coverage, and the plots obtained are presented in Figure 7A.

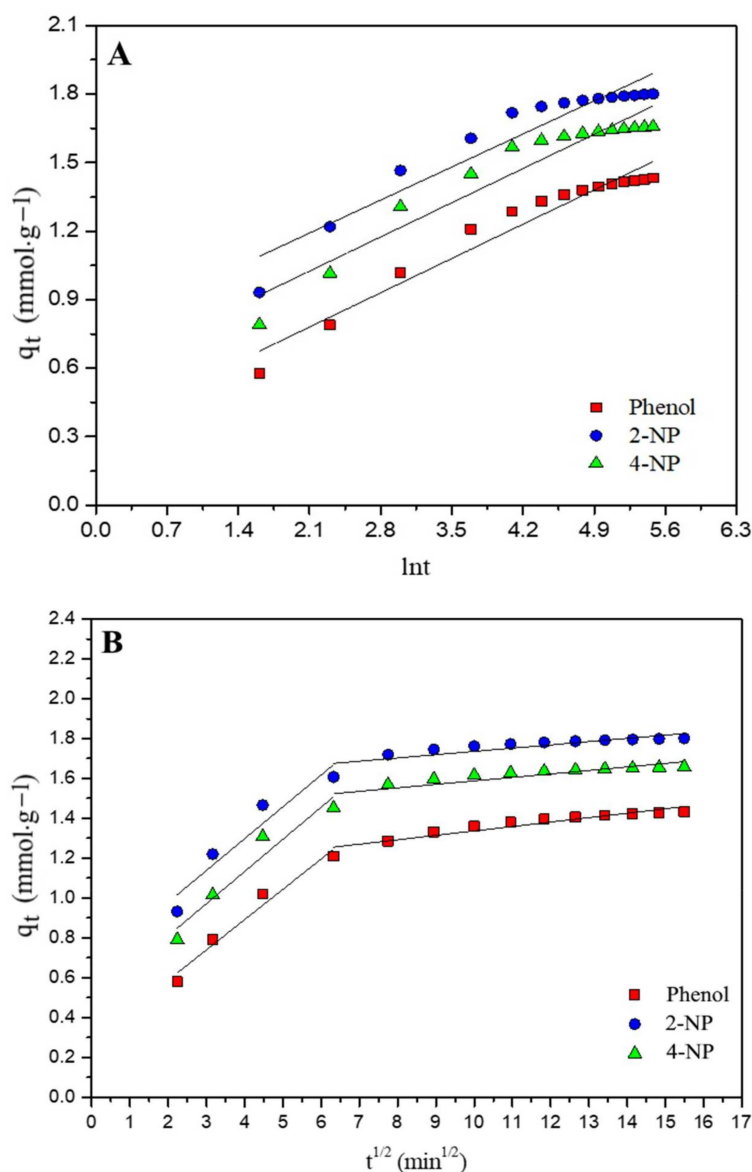


Figure 7. Elovich (A) and IPD (B) kinetic plots for the removal of phenol, 2-NP, and 4-NP by DKLAAC at 25 °C with phenol concentration at $2 \times 10^{-3} \text{ mol}\cdot\text{L}^{-1}$.

The results obtained from these kinetic models are shown in Table 5. It was found that the PSO model has better R^2 values and therefore fits best to the adsorption data of phenol

and NPs as compared with the PFO and Elovich models, which are similar to the findings reported for adsorption of phenols by *Luffa cylindrica* [44].

In order to investigate the rate-controlling mechanism and to understand the adsorption process more precisely, the equilibrium data were also validated using an intraparticle diffusion model (IPD) model [69]. Out of the four steps commonly involved in the adsorption process, the first and last step [70] are usually very fast and account for the migration of adsorbate (phenols) from the liquid to the adsorbent (DKLAAC) surface. The second and third steps account for the diffusion of adsorbate molecules (phenols) and are considered as rate-controlling steps either alone or in combination. The rate constants for using the IPD model can be calculated with the following expression (Equation (13)):

$$q_t = K_{id} \cdot t^{1/2} + C \quad (13)$$

where K_{id} is the rate constant and C is a constant corresponding to the thickness of the boundary layer. Plots between q_t and $t^{1/2}$ were made for the analysis of the adsorptive removal of phenol and NPs (Figure 7B). The Figure 7B consists of two linear sections with film diffusion and IPD as the first and second steps, respectively. The intra particle rate constants K_{id} (K_{id1} for the 1st step and K_{id2} for the 2nd step) and C (C_1 for the 1st step and C_2 for the 2nd step) values were evaluated from these linear parts of the plots and are shown in Table 5. As is clear from the Figure 7B, the straight line does not pass through the origin, and it can be collectively deduced that the adsorption of phenol, 2-NP, and 4-NP onto DKLAAC is a complex process involving a combination of IPD and surface sorption in the rate-limiting step of the adsorption process [44].

4. Conclusions

This work was carried out to investigate the impact of the nitro groups and to know the role of their position on the adsorption of phenol, 2-NP, and 4-NP on DKLAAC. The interaction and position of nitro groups present on the phenol play a crucial role in their adsorption and it was found that nitro groups (deactivating group) would increase the extent of adsorption via the electron donor–acceptor mechanism and the hydrophobicity of the adsorbate. Interestingly, the hydrophobicity factor promotes the adsorption of NPs as it was found that 2-NP possessing the least solubility (more hydrophobicity) adsorbed to a greater extent than 4-NP and phenol. The experimental adsorption capacities were found to be 2.09, 2.34, and 2.20 mmol·g⁻¹ respectively for phenol, 2-NP, and 4-NP on DKLAAC, following the order 2-NP > 4-NP > phenol at 25 °C. The experimental data were best described using the Langmuir isotherm and an increase in the adsorption of phenols on raising the temperature from 25 °C to 45 °C indicated the process to be endothermic. The thermodynamic parameters could well-describe the spontaneity and favorability of the adsorption process. The negative values of ΔG° suggested that the adsorption process was governed by physisorption, while small positive ΔH° values indicated the endothermic and physisorption nature of the adsorption process. Moreover, the high affinity for removal of phenols by DKLAAC was revealed by the positive value of ΔS° . A pseudo second-order model was found to precisely describe the kinetic data.

Supplementary Materials: The following supporting information can be downloaded at: <https://www.mdpi.com/article/10.3390/agronomy12102564/s1>, Figure S1: Effect of initial concentration for the removal of phenol by demineralized kraft lignin activated carbon (DKLAAC) at different initial concentrations at 25 °C; Figure S2: Effect of initial concentration for the removal of 4-nitrophenol (4-NP) by DKLAAC at different initial concentrations at 25 °C; Figure S3: Effect of pH on the adsorption of Phenol, 2-NP and 4-NP on DKLAAC at 25 °C with initial phenol concentration at 1×10^{-3} M; Figure S4: Langmuir adsorption isotherms of phenol on DKLAAC at different temperatures; Figure S5: Langmuir adsorption isotherms of 4-NP on DKLAAC at different temperatures; Figure S6: Freundlich adsorption isotherms of phenol on DKLAAC at different temperatures; Figure S7: Freundlich adsorption isotherms of 4-NP on DKLAAC at different temperatures; Figure S8: Temkin adsorption isotherms of phenol on DKLAAC at different temperatures; Figure S9: Temkin

adsorption isotherms of 4-NP on DKLAAC at different temperatures; Figure S10: D-R adsorption isotherms of phenol on DKLAAC at different temperatures; Figure S11: D-R adsorption isotherms of 4-NP on DKLAAC at different temperatures.

Author Contributions: Conceptualization, S. and M.C.; methodology, M.C. and S.; software, S., M.C., B.S.I., and M.S.; validation, M.C., S.K., J.G., S.C., M.S., and S.; formal analysis, M.C., S.C., and S.; investigation, M.C., S.K., and S.; resources, M.C. and S.; data curation, S., M.C., B.S.I., and M.S.; writing—original draft, M.C. and S.; writing—review and editing, M.C., J.G., S.C., I.T., M.H.D., B.S.I., and S.; visualization, M.C., J.G., M.H.D., S.C., I.T., B.S.I., and S.; supervision, S. All authors have read and agreed to the published version of the manuscript.

Funding: This research received no external funding.

Data Availability Statement: All data generated or analyzed during this study are included in this article.

Acknowledgments: Authors are thankful to DST, New Delhi, India. Author (Monika Chaudhary INSPIRE Fellow code IF120368) is grateful to the DST (Department of Science and Technology), New Delhi, India for the award of a doctoral grant (No. DST/INSPIRE Fellowship/2012/346).

Conflicts of Interest: The authors declare no conflict of interest.

References

1. Ali, I.; Asim, M.; Khan, T.A. Low cost adsorbents for the removal of organic pollutants from wastewater. *J. Environ. Manag.* **2012**, *113*, 170–183. [CrossRef] [PubMed]
2. Yang, M. A current global view of environmental and occupational cancers. *J. Environ. Sci. Health C Environ. Carcinog. Ecotoxicol. Rev.* **2011**, *29*, 223–249. [CrossRef] [PubMed]
3. US EPA. Toxic and Priority Pollutants Under the Clean Water Act. US EPA. Available online: <https://www.epa.gov/eg/toxic-and-priority-pollutants-under-clean-water-act> (accessed on 24 January 2021).
4. Honarmandrad, Z.; Javid, N.; Malakootian, M. Removal efficiency of phenol by ozonation process with calcium peroxide from aqueous solutions. *Appl. Water Sci.* **2021**, *11*, 14. [CrossRef]
5. Yang, S.; Chen, D.; Li, N.; Xu, Q.; Li, H.; He, J.; Lu, J. Surface-Nanoengineered Bacteria for Efficient Local Enrichment and Biodegradation of Aqueous Organic Wastes: Using Phenol as a Model Compound. *Adv. Mater.* **2016**, *28*, 2916–2922. [CrossRef] [PubMed]
6. Heitkamp, M.A.; Camel, V.; Reuter, T.J.; Adams, W.J. Biodegradation of p-nitrophenol in an aqueous waste stream by immobilized bacteria. *Appl. Environ. Microbiol.* **1990**, *56*, 2967–2973. [CrossRef]
7. Kadam, H.K.; Tilve, S.G. Advancement in methodologies for reduction of nitroarenes. *RSC Adv.* **2015**, *5*, 83391–83407. [CrossRef]
8. Ma, Y.; Ma, Y.; Gao, N.; Chu, W.; Li, C. Removal of phenol by powdered activated carbon adsorption. *Front. Environ. Sci. Eng.* **2013**, *7*, 158–165. [CrossRef]
9. Adebayo, M.A.; Areo, F.I. Removal of phenol and 4-nitrophenol from wastewater using a composite prepared from clay and Cocos nucifera shell: Kinetic, equilibrium and thermodynamic studies. *Resour. Environ. Sustain.* **2021**, *3*, 100020. [CrossRef]
10. Khalid, M.; Joly, G.; Renaud, A.; Magnoux, P. Removal of Phenol from Water by Adsorption Using Zeolites. *Ind. Eng. Chem. Res.* **2004**, *43*, 5275–5280. [CrossRef]
11. Liu, B.; Yang, F.; Zou, Y.; Peng, Y. Adsorption of Phenol and p-Nitrophenol from Aqueous Solutions on Metal–Organic Frameworks: Effect of Hydrogen Bonding. *J. Chem. Eng. Data* **2014**, *59*, 1476–1482. [CrossRef]
12. Sarker, N.; Fakhruddin, A.N.M. Removal of phenol from aqueous solution using rice straw as adsorbent. *Appl. Water Sci.* **2017**, *7*, 1459–1465. [CrossRef]
13. Castillejos-López, E.; Nevskaja, D.M.; Muñoz, V.; Guerrero-Ruiz, A. On the interactions of phenol, aniline and p-nitrophenol on activated carbon surfaces as detected by TPD. *Carbon* **2008**, *46*, 870–875. [CrossRef]
14. Qu, G.; Liang, D.; Qu, D.; Huang, Y.; Liu, T.; Mao, H.; Ji, P.; Huang, D. Simultaneous removal of cadmium ions and phenol from water solution by pulsed corona discharge plasma combined with activated carbon. *Chem. Eng. J.* **2013**, *228*, 28–35. [CrossRef]
15. Robau-Sánchez, A.; Aguilar-Elguézabal, A.; de la Torre-Sáenz, L.; Lardizábal-Gutiérrez, D. Radial distribution of porosity in spherical activated carbon particles. *Carbon* **2003**, *41*, 693–698. [CrossRef]
16. Chaudhary, M.; Suhas; Singh, R.; Tyagi, I.; Ahmed, J.; Chaudhary, S.; Kushwaha, S. Microporous activated carbon as adsorbent for the removal of noxious anthraquinone acid dyes: Role of adsorbate functionalization. *J. Environ. Chem. Eng.* **2021**, *9*, 106308. [CrossRef]
17. Asgharnia, H.; Nasehinia, H.; Rostami, R.; Rahmani, M.; Mehdinia, S.M. Phenol removal from aqueous solution using silica and activated carbon derived from rice husk. *Water Pract. Technol.* **2019**, *14*, 897–907. [CrossRef]
18. Faisal, A.; Daud, W.M.A.W.; Ahmad, M.A.; Radzi, R. Using cocoa (*Theobroma cacao*) shell-based activated carbon to remove 4-nitrophenol from aqueous solution: Kinetics and equilibrium studies. *Chem. Eng. J.* **2011**, *178*, 461–467. [CrossRef]

19. Yahya, A.A.; Rashid, K.T.; Ghadhban, M.Y.; Mousa, N.E.; Majdi, H.S.; Salih, I.K.; Alsahy, Q.F. Removal of 4-Nitrophenol from Aqueous Solution by Using Polyphenylsulfone-Based Blend Membranes: Characterization and Performance. *Membranes* **2021**, *11*, 171. [[CrossRef](#)]
20. Allen, S.J.; Koumanova, B.; Kircheva, Z.; Nenkova, S. Adsorption of 2-nitrophenol by technical hydrolysis lignin: Kinetics, mass transfer, and equilibrium studies. *Ind. Eng. Chem. Res.* **2005**, *44*, 2281–2287. [[CrossRef](#)]
21. Jaoui, M.; Achard, C.; Rogalski, M. Solubility as a function of temperature of selected chlorophenols and nitrophenols in aqueous solutions containing electrolytes or surfactants. *J. Chem. Eng. Data* **2002**, *47*, 297–303. [[CrossRef](#)]
22. Jain, A.K.; Gupta, V.K.; Jain, S.; Suhas. Removal of Chlorophenols Using Industrial Wastes. *Environ. Sci. Technol.* **2004**, *38*, 1195–1200. [[CrossRef](#)]
23. Suhas; Carrott, P.; Carrott, M.R.; Singh, R.; Singh, L.; Chaudhary, M. An innovative approach to develop microporous activated carbons in oxidising atmosphere. *J. Clean. Prod.* **2017**, *156*, 549–555. [[CrossRef](#)]
24. Albadarin, A.B.; Collins, M.N.; Naushad, M.; Shirazian, S.; Walker, G.; Mangwandi, C. Activated lignin-chitosan extruded blends for efficient adsorption of methylene blue. *Chem. Eng. J.* **2017**, *307*, 264–272. [[CrossRef](#)]
25. Fu, J.; Xin, Q.; Wu, X.; Chen, Z.; Yan, Y.; Liu, S.; Wang, M.; Xu, Q. Selective adsorption and separation of organic dyes from aqueous solution on polydopamine microspheres. *J. Colloid Interface Sci.* **2016**, *461*, 292–304. [[CrossRef](#)]
26. Mojoudi, N.; Mirghaffari, N.; Soleimani, M.; Shariatmadari, H.; Belver, C.; Bedia, J. Phenol adsorption on high microporous activated carbons prepared from oily sludge: Equilibrium, kinetic and thermodynamic studies. *Sci. Rep.* **2019**, *9*, 19352. [[CrossRef](#)]
27. Zhang, J. Phenol Removal from Water with Potassium Permanganate Modified Granular Activated Carbon. *J. Environ. Prot.* **2013**, *4*, 411–417. [[CrossRef](#)]
28. Zhang, J.; Chen, S.; Zhang, H.; Wang, X. Removal behaviors and mechanisms of hexavalent chromium from aqueous solution by cephalosporin residue and derived chars. *Bioresour. Technol.* **2017**, *238*, 484–491. [[CrossRef](#)]
29. Aksu, Z.; Akin, A.B. Comparison of Remazol Black B biosorptive properties of live and treated activated sludge. *Chem. Eng. J.* **2010**, *165*, 184–193. [[CrossRef](#)]
30. Ayranci, E.; Duman, O. Adsorption behaviors of some phenolic compounds onto high specific area activated carbon cloth. *J. Hazard. Mater.* **2005**, *124*, 125–132. [[CrossRef](#)]
31. Cotoruelo, L.; Marqués, M.D.; Díaz, F.J.; Rodríguez-Mirasol, J.; Rodríguez, J.J.; Cordero, T. Adsorbent ability of lignin-based activated carbons for the removal of p-nitrophenol from aqueous solutions. *Chem. Eng. J.* **2012**, *184*, 176–183. [[CrossRef](#)]
32. Rani, S.; Sumanjit, K.; Mahajan, R. Comparative study of surface modified carbonized Eichhornia crassipes for adsorption of dye safranin. *Sep. Sci. Technol.* **2015**, *50*, 2436–2447.
33. Sun, X.; Cheng, P.; Wang, H.; Xu, H.; Dang, L.; Liu, Z.; Lei, Z. Activation of graphene aerogel with phosphoric acid for enhanced electrocapacitive performance. *Carbon* **2015**, *92*, 1–10. [[CrossRef](#)]
34. Yu, M.; Han, Y.; Li, J.; Wang, L. CO₂-activated porous carbon derived from cattail biomass for removal of malachite green dye and application as supercapacitors. *Chem. Eng. J.* **2017**, *317*, 493–502. [[CrossRef](#)]
35. Sözüdoğru, O.; Fil, B.A.; Boncukcuoğlu, R.; Aladağ, E.; Kul, S. Adsorptive removal of cationic (BY2) dye from aqueous solutions onto Turkish clay: Isotherm, kinetic, and thermodynamic analysis. *Part. Sci. Technol.* **2016**, *34*, 103–111. [[CrossRef](#)]
36. Cotoruelo, L.M.; Marqués, M.D.; Díaz, F.J.; Rodríguez-Mirasol, J.; Rodríguez, J.J.; Cordero, T. Lignin-based activated carbons as adsorbents for crystal violet removal from aqueous solutions. *Environ. Prog. Sustain. Energy* **2012**, *31*, 386–396. [[CrossRef](#)]
37. Qiao, B. A combined experiment and molecular dynamics simulation study of hydrogen bonds and free volume in nitrile-butadiene rubber/hindered phenol damping mixtures. *J. Mater. Chem.* **2012**, *22*, 12339–12348. [[CrossRef](#)]
38. Selvaraj, R.; Moon, S.-H.; Sivabalan, R.; Arabindoo, B.; Murugesan, V. Removal of phenol from aqueous solution and resin manufacturing industry wastewater using an agricultural waste: Rubber seed coat. *J. Hazard. Mater.* **2002**, *89*, 185–196.
39. Langmuir, I. The adsorption of gases on plane surfaces of glass, mica and platinum. *J. Am. Chem. Soc.* **1918**, *40*, 1361–1403. [[CrossRef](#)]
40. Freundlich, H. Over the adsorption in solution. *J. Phys. Chem.* **1906**, *57*, 1100–1107.
41. Temkin, M. Kinetics of ammonia synthesis on promoted iron catalysts. *Acta Physicochim. URSS* **1940**, *12*, 327–356.
42. Dubinin, M.M. The Equation of the Characteristic Curve of Activated Charcoal. *Proc. USSR Acad. Sci.* **1947**, *55*, 327–329.
43. Rincón-Silva, N.G.; Moreno-Piraján, J.C.; Giraldo, L.G. Thermodynamic Study of Adsorption of Phenol, 4-Chlorophenol, and 4-Nitrophenol on Activated Carbon Obtained from Eucalyptus Seed. *J. Chem.* **2015**, *2015*, 569403. [[CrossRef](#)]
44. Salimi, M.; Salehi, Z.; Heidari, H.; Vahabzadeh, F. Production of activated biochar from *Luffa cylindrica* and its application for adsorption of 4-Nitrophenol. *J. Environ. Chem. Eng.* **2021**, *9*, 105403. [[CrossRef](#)]
45. Dąbrowski, A.; Podkościelny, P.; Hubicki, Z.; Barczak, M. Adsorption of phenolic compounds by activated carbon—A critical review. *Chemosphere* **2005**, *58*, 1049–1070. [[CrossRef](#)]
46. Supong, A.; Bhomick, P.C.; Karmaker, R.; Ezung, S.L.; Jamir, L.; Sinha, U.B.; Sinha, D. Experimental and theoretical insight into the adsorption of phenol and 2, 4-dinitrophenol onto *Tithonia diversifolia* activated carbon. *Appl. Surf. Sci.* **2020**, *529*, 147046. [[CrossRef](#)]
47. Mattson, J.A.; Mark Jr, H.B.; Malbin, M.D.; Weber Jr, W.J.; Crittenden, J.C. Surface chemistry of active carbon: Specific adsorption of phenols. *J. Colloid Interface Sci.* **1969**, *31*, 116–130. [[CrossRef](#)]

48. Cotoruelo, L.; Marqués, M.; Leiva, A.; Rodríguez-Mirasol, J.; Cordero, T. Adsorption of oxygen-containing aromatics used in petrochemical, pharmaceutical and food industries by means of lignin based active carbons. *Adsorption* **2011**, *17*, 539–550. [[CrossRef](#)]
49. Lua, A.C. A detailed study of pyrolysis conditions on the production of steam-activated carbon derived from oil-palm shell and its application in phenol adsorption. *Biomass Convers. Biorefinery* **2020**, *10*, 523–533. [[CrossRef](#)]
50. Lütke, S.F.; Igansi, A.V.; Pegoraro, L.; Dotto, G.L.; Pinto, L.A.A.; Cadaval, T.R.S. Preparation of activated carbon from black wattle bark waste and its application for phenol adsorption. *J. Environ. Chem. Eng.* **2019**, *7*, 103396. [[CrossRef](#)]
51. Hameed, B.H.; Rahman, A.A. Removal of phenol from aqueous solutions by adsorption onto activated carbon prepared from biomass material. *J. Hazard. Mater.* **2008**, *160*, 576–581. [[CrossRef](#)]
52. Kumar, A.; Kumar, S.; Kumar, S.; Gupta, D.V. Adsorption of phenol and 4-nitrophenol on granular activated carbon in basal salt medium: Equilibrium and kinetics. *J. Hazard. Mater.* **2007**, *147*, 155–166. [[CrossRef](#)] [[PubMed](#)]
53. Rincón-Silva, N.G.; Moreno-Piraján, J.C.; Giraldo, L. Equilibrium, kinetics and thermodynamics study of phenols adsorption onto activated carbon obtained from lignocellulosic material (*Eucalyptus globulus* Labill seed). *Adsorption* **2016**, *22*, 33–48. [[CrossRef](#)]
54. Mohammadi, S.Z.; Darijani, Z.; Karimi, M.A. Fast and efficient removal of phenol by magnetic activated carbon-cobalt nanoparticles. *J. Alloys Compd.* **2020**, *832*, 154942. [[CrossRef](#)]
55. Silva, N.F.; Netto, M.S.; Silva, L.F.O.; Mallmann, E.S.; Lima, E.C.; Ferrari, V.; Dotto, G.L. Composite carbon materials from winery composted waste for the treatment of effluents contaminated with ketoprofen and 2-nitrophenol. *J. Environ. Chem. Eng.* **2021**, *9*, 105421. [[CrossRef](#)]
56. Magdy, Y.M.; Altaher, H.; ElQada, E. Removal of three nitrophenols from aqueous solutions by adsorption onto char ash: Equilibrium and kinetic modeling. *Appl. Water Sci.* **2018**, *8*, 26. [[CrossRef](#)]
57. Isichei, T.; Okieimen, F. Adsorption of 2-Nitrophenol onto Water Hyacinth Activated Carbon-Kinetics and Equilibrium Studies. *Environ. Pollut.* **2014**, *3*, 99–111. [[CrossRef](#)]
58. Arasteh, R.; Masoumi, M.; Rashidi, A.M.; Moradi, L.; Samimi, V.; Mostafavi, S.T. Adsorption of 2-nitrophenol by multi-wall carbon nanotubes from aqueous solutions. *Appl. Surf. Sci.* **2010**, *256*, 4447–4455. [[CrossRef](#)]
59. Wasilewska, M.; Marczewski, A.W.; Deryło-Marczewska, A.; Sternik, D. Nitrophenols removal from aqueous solutions by activated carbon—Temperature effect of adsorption kinetics and equilibrium. *J. Environ. Chem. Eng.* **2021**, *9*, 105459. [[CrossRef](#)]
60. Renault, F.; Morin-Crini, N.; Gimbert, F.; Badot, P.-M.; Crini, G. Cationized starch-based material as a new ion-exchanger adsorbent for the removal of C.I. Acid Blue 25 from aqueous solutions. *Bioresour. Technol.* **2008**, *99*, 7573–7586. [[CrossRef](#)] [[PubMed](#)]
61. Mu'azu, N.D.; Zubair, M.; Ihsanullah, I. Process Optimization and Modeling of Phenol Adsorption onto Sludge-Based Activated Carbon Intercalated MgAlFe Ternary Layered Double Hydroxide Composite. *Molecules* **2021**, *26*, 4266. [[CrossRef](#)]
62. Umpierrez, C.S.; Thue, P.S.; Lima, E.C.; Reis, G.S.d.; de Brum, I.A.S.; de Alencar, W.S.; Dias, S.L.P.; Dotto, G.L. Microwave-activated carbons from tucumã (*Astrocaryum aculeatum*) seed for efficient removal of 2-nitrophenol from aqueous solutions. *Environ. Technol.* **2018**, *39*, 1173–1187. [[CrossRef](#)] [[PubMed](#)]
63. Liu, L.; Deng, G.; Shi, X. Adsorption characteristics and mechanism of p-nitrophenol by pine sawdust biochar samples produced at different pyrolysis temperatures. *Sci. Rep.* **2020**, *10*, 5149. [[CrossRef](#)] [[PubMed](#)]
64. Dhorabe Prashant, T.; Lataye Dilip, H.; Ingole Ramakant, S. Adsorptive Removal of 4-Nitrophenol from Aqueous Solution by Activated Carbon Prepared from Waste Orange Peels. *J. Hazard. Toxic Radioact. Waste* **2017**, *21*, 04016015. [[CrossRef](#)]
65. Achari, V.S.; Jayasree, S.; Rajalakshmi, A. Adsorption of p-nitrophenol on coconut shell granular activated carbon: Isotherms, kinetics and thermodynamics. *Indian J. Chem. Technol.* **2018**, *24*, 471–478.
66. Lagergren, S. About the theory of so-called adsorption of soluble substances. *K. Sven. Vetensk. Handl.* **1898**, *24*, 1–39.
67. Ho, Y.-S.; McKay, G. Sorption of dye from aqueous solution by peat. *Chem. Eng. J.* **1998**, *70*, 115–124. [[CrossRef](#)]
68. Elovich, S. *Proceedings of the Second International Congress on Surface Activity*; Academic Press Inc.: New York, NY, USA, 1959.
69. Weber, W.; Morris, J. Advances in water pollution research. In *Proceedings of the First International Conference on Water Pollution Research*; Pergamon Press: Oxford, UK, 1962.
70. Weber, W.J., Jr. Evolution of a technology. *J. Environ. Eng.* **1984**, *110*, 899–917. [[CrossRef](#)]